

The direct Monte Carlo method applied to the homogeneous nucleation problem

Hinne Hetteema and John S. McFeaters

*Computational Materials Science and Engineering Research Centre, University of Auckland,
Private Bag 92019, Auckland, New Zealand*

(Received 23 January 1996; accepted 9 May 1996)

We discuss the application of the direct Monte Carlo method to the theory of cluster formation. Fractal relationships for the kernels appearing in the Smoluchowski equation are implemented in this method and the scaling behavior of the kernels is investigated using computer simulation. We study the effects of cluster disintegrations and also investigate the effects of “magic” numbers in cluster formation. © 1996 American Institute of Physics. [S0021-9606(96)51231-6]

I. INTRODUCTION

The theory of homogeneous nucleation has recently attracted renewed interest. In classical homogeneous nucleation theory the onset of nucleation is characterized by the formation of significant numbers of thermodynamically stable clusters of monomers. Such clusters are, in a sense, a new phase of the material, which exhibit quite specific properties of their own.^{1,2} A good overview of the current research on clusters is given in the recent collection of papers edited by Haberland.³

Cluster formation is of immediate scientific and technological importance. For instance in chemical vapor deposition processes, the properties of the surface can be affected by cluster formation and part of the deposition process is known to proceed via cluster formation.⁴ In the dry etching of silicon wafers cluster formation in the plasma can foul the surface, leading to manufacturing irregularities.⁵ The phenomenon of quantum dots⁶ can also be viewed as a cluster phenomenon. Small quantities of material are embedded in a host material, and their “cluster” properties lead specifically to the electrical and optical properties of the quantum dot. The theory of the processing of nanoscale materials is often based on homogeneous nucleation theory and the formation of soot and atmospheric pollutants often begins with formation of clusters. Furthermore, the role of clusters as catalysts for chemical reactions is starting to be recognized.⁷

Theoretically, atomic clusters are interesting in their own right. They represent a very special area in physics because they bridge the gap between the microscopic and the macroscopic world. A monomer’s behavior is governed by atomic and molecular mechanics while the behavior of the bulk material is governed by the macroscopic qualities of the material. As clusters form and grow, their behavior develops from the molecular to the bulk behavior in a semi-continuous fashion. The traditional definition of a “phase” has limited meaning with respect to clusters. Solids for instance are characterized by long range order and similarly liquids by short range order. However, with the nascent clusters, the characteristic dimensions are often very different from the characteristic lengths for either long or short range order and their properties are often dominated by surface effects. The theory of formation of clusters from monomers (nucleation theory)

is a field of study, where (molecular) dynamics, statistical thermodynamics and chemical reaction theory intersect.

Under some circumstances, clusters exhibit an electronic shell structure not unlike the atomic model of Thomson, leading to “magic numbers” in the occurrence of clusters of a certain size. At the magic numbers there are shell closings of the electronic structure and the “closed shell” clusters display anomalous stabilities.^{8,9} The “open shell” clusters exhibit geometrical distortions of a Jahn–Teller type, leading to considerable changes in the overall shape of the cluster as a function of the number of monomers. These anomalies have consequences for the size distribution of the clusters and are known to be influential even for high cluster numbers.

Much of the work in the area of cluster formation derives from the original treatment given by Gibbs, Thomson and Helmholtz.¹⁰ The process has been discussed in relation to phase transitions by Fisher.¹¹ Two approaches to homogeneous nucleation exist in the literature. Though there is considerable overlap between the two, historically one approach originates in the work by Zeldovitch and Becker and Döring,¹² the other in the work of Smoluchowski¹³ on emulsification. For the purpose of this paper, we will designate the first approach as “classical nucleation theory” (CNT) and the second, the “kinetic” approach. Though some aspects of the approaches are very similar, up to now they have been used in different contexts and have generated rather different lines of research. Part of this paper is devoted to a study of their similarities and differences.

In the classical approach it is assumed that the cluster formation proceeds with one monomer at a time. In the initial stages of the aggregation process this leads to a barrier in the free energy, which occurs at a certain critical cluster size i^* . This critical size functions as a transition state: clusters smaller than the critical size are unstable with respect to reversion to the vapor, clusters larger than the critical size grow irreversibly, ultimately forming the condensed phase. The critical size is the smallest number of monomers which can form a thermodynamically stable cluster. This is typically on the order of 10 to 100 monomers. Below this size

the clusters tend to spontaneously decompose. The clusters A_{i^*} thus serve as the “transition state” in the nucleation process. A “rate constant” for cluster formation can then be derived in terms of this transition state as^{14,15}

$$J_{cl} = C n_1 \exp\left[\frac{-\Delta G_{i^*}}{kT}\right]. \quad (1.1)$$

At equilibrium, J_{cl} is constant since the rate of formation is matched by the rate of loss and we obtain the nucleation rate for CNT^{16–18}

$$J = \frac{N\beta s_1}{3} \left(\frac{\Theta}{\pi}\right)^{1/2} \exp\left[-\frac{4}{27} \frac{\Theta^3}{(\ln S)^2}\right], \quad (1.2)$$

where $\Theta = \sigma s_1 / k_B T$, σ is the (bulk value of the) surface tension, s_1 is the surface of a monomer, k_B is Boltzmann's constant, S is the monomer supersaturation, β is the monomer flux to the surface and T is the temperature in Kelvin. In the original version of CNT, growth and depletion of the clusters was assumed to proceed one monomer at a time.^{12,19,16} This approximation, which does not allow for agglomeration in the formation of critical sized clusters, has been investigated,²⁰ and was recently shown to be justifiable.²¹ It should also be noted that this line of research on cluster formation has led to a “kinetic” approach.¹⁶ Practical applications of the CNT equation for nucleation give results which in general are qualitatively correct but require a multiplicative correction factor to predict quantitative behavior. This correction factor (“replacement factor”), principally accounts for the fact that the equation for the free energy is not consistent as $i \rightarrow 1$. A number of researchers have proposed correction factors and functional corrections.^{17,18,22,23}

As can be seen from Eq. (1.1) the key aspect in the CNT approach is the free energy of the cluster and the concomitant problem of finding an expression for the surface tension of the cluster as a function of cluster size.²² For very small droplets, the value for the surface tension deviates significantly, but in a largely unknown fashion, from the bulk value.²³ Apart from the uncertainties in the properties of small clusters used in this approach, another problem is that the final expression yields only limited information about cluster formation and can be difficult to implement in practical cases. Also, on its own, the CNT expression gives no information on the cluster size distribution or structure.

In the second approach to cluster formation, which we refer to as the “kinetic” approach in this paper, “nucleation” is viewed as a process of chemical aggregation. The original equation for this approach is the Smoluchowski equation.^{13,24–27} This approach gives an insight into the dynamical aspects of cluster formation and has recently attracted a lot of interest in the literature on fractals.^{28–30} The chemical reaction rate constants $K_T(i, j)$ used in the rate equation (called the “kernels” in the fractal literature) are assumed to have “fractal” (non-integer) scaling properties with cluster size

$$K_T(\lambda i, \lambda j) = \lambda^{2\omega} K_T(i, j), \quad (1.3)$$

where 2ω is a non-integer number, and the subscript T refers to the temperature dependence. The kinetics of cluster formation can be studied as a function of the fractality of the kernels. The Smoluchowski equation leads to a set of time-dependent coupled differential equations, that can be solved numerically on a computer (see for instance Refs. 25 and 26). Alternatively, the cluster formation process may be simulated using a suitable direct simulation method and the same results should be obtained in principle.

In this paper we will show that fractal scaling of kernels can be implemented in the *direct Monte Carlo* (DMC) simulation method in a straightforward fashion. This method was pioneered by Bird³¹ and later used by Anderson^{32–34} in studies of chemical kinetics of model systems. The method is comparatively fast, easy to implement and yields good results for model systems. The advantage of the DMC procedure is that the kernels of the Smoluchowski equation can be directly related to the quantities $v\sigma_R$ (where v is the relative velocity and σ_R the reactive cross section) that determine the reaction probabilities in the direct Monte Carlo method

$$K_T(i, j) \approx \langle v_{rel}(i, j) \sigma_R(i, j) \rangle_T. \quad (1.4)$$

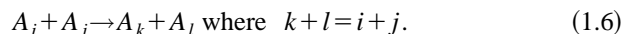
The DMC method is not specific to the functional form of the reaction cross sections σ_R so that we may choose any reasonable way to treat the collision dynamics. This makes it possible to test some of the laws relating to cluster formation using numerical simulation.

The material in this paper is complementary to the material in the recent paper of Venkatesh *et al.*,³⁵ in which the thermal collision rate constants for small nickel clusters (2–14 atoms) were calculated. The aim of their paper was to investigate the validity of the simplifying assumptions that are often used in models of cluster growth and provide additional information on the breakdown of their validity. Specifically, they distinguish four types of cluster reactions:

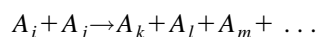
(i) Simple (elastic) collisions, where the clusters remain unaltered,



(ii) Stripping or rearrangement,



(iii) Fragmentation or dissociation,



$$\text{where } i + j = k + l + m + \dots \quad (1.7)$$

(iv) Sticking,



With the exception of (iii), our DMC method incorporates all of these cluster processes.

II. THEORY

In this section, we discuss the application of Anderson's direct Monte Carlo (DMC) method to the process of homogeneous nucleation. We first summarize some aspects of two kinetic theories of cluster formation: classical nucleation theory and the Smoluchowski theory. Both theories are very similar from a mathematical point of view, but different in aim and scope. In the classical nucleation theory the aim is to derive an expression for the nucleation rate J , the rate with which nuclei (clusters of the minimum stable size) form in a condensing species. The concept of an "equilibrium state" plays a central role in CNT as the connection between free energy and kinetics in the determination of the nucleation rate. The Smoluchowski equation does not invoke the concept of an "equilibrium state." Rather it is a dynamical equation that describes coagulation and clustering phenomena. It is of interest because of the fractal scaling theory of the kernels. It is this scaling behavior of the kernels that leads to an immediate characterization of the clustering process. In this section, we also discuss the central results of this theory, and we then go on to discuss some central equations from the distribution theory of cluster formation. At each moment in time, we can characterize the nucleating system by the parameters of its distribution of cluster sizes, typically the log normal distribution.

Then we discuss the implementation of the homogeneous nucleation process into the DMC method. It will be shown that the DMC method can easily incorporate most aspects of the fractal theory of clusters in terms of a physical model. These results can furthermore be translated into terms of the kinetic models discussed earlier and thus serve as tests of these models.

A. Two kinetic theories of cluster formation

As with all approaches, we start with a system consisting of N monomers. We designate a cluster of "size" k (cluster with k monomers) by A_k and the number of such clusters by n_k . The time variable is denoted by t .

1. Classical nucleation theory

We include only a brief discussion of classical nucleation theory here. The theory is obtained^{16,20} when aggregation is assumed to take place with one monomer at a time. The rate of formation of clusters with k monomers is then expressed in terms of a "forward" rate constant $f(k,t)$ and a "backward" rate constant $b(k+1)$. Then (see for instance Refs. 16 and 17) we introduce the concept of a "steady" or "equilibrium state" and use detailed balance to express the "backward" rate constant $b(k+1)$ in terms of the equilibrium values of the forward rate constant and the cluster concentrations. Two further mathematical tricks, as explained in for instance Refs. 16 and 17, lead to the expression Eq. (1.2). The concept of the "equilibrium state," where the nucleation rate is constant and independent of cluster size is central to all derivations of CNT.

2. Smoluchowski approach

In the Smoluchowski approach the basic equation for the kinetic theory (the Smoluchowski equation) is the equation describing the rate of cluster formation and depletion

$$\frac{dn_k}{dt} = \frac{1}{2} \sum_{i+j=k} K(i,j)n_i n_j - n_k \sum_{i=1}^{\infty} K(i,k)n_i, \quad (2.1)$$

where we have neglected dissociation of clusters into smaller clusters. The first term represents the rate of creation of A_k through association with smaller clusters, the last term the loss of clusters A_k through chemical reactions with other clusters. The second term in Eq. (2.1) includes both rearrangement and dissociation [expressions (1.6) and (1.7)]. However, in this paper we neglect the dissociation of clusters. This assumption implies that the results obtained apply to what Rao and McMurry³⁶ refer to as the collision controlled regime where the rate of growth is limited by the collision frequency rather than the balance between growth and decay. The dissociation or fragmentation of clusters can be included in the DMC method. However, an independent criteria must be developed to parametrize the rates for the "reverse" step because this method does not include the assumption of an equilibrium state so that the principle of detailed balance cannot be invoked to relate forward and backward rates. The relaxation of the equilibrium assumption is also one of the advantages of this method. However, the implementation of these effects is beyond the scope of this paper. The efficiency of the "chemical" reactions between clusters and individual atoms or clusters of different size is given by the chemical reaction rate coefficients K . In the fractal literature relating to this approach, the K 's are referred to as the "kernels" and the scaling behavior of the kernels (as a function of cluster size) is investigated.

In the original Smoluchowski paper,²⁴ all kernels were assumed to have a constant value for K ; with this approximation, the equation can be solved exactly (see Ref. 30 for instance) and the number of clusters of size k at time t , $n_k(t)$, is given by²⁴

$$n_k(t) = \frac{N[(1/2)KNt]^{k-1}}{[1+(1/2)KNt]^{k+1}}. \quad (2.2)$$

The total number of clusters at time t , $N_C(t)$ is given by

$$N_C(t) = \frac{N}{[1+(KN/2)t]}. \quad (2.3)$$

The Smoluchowski equation as given above is still a simplification since it does not allow for the disintegration of a cluster A_{i+j} into $A_i + A_j$. Cluster disintegration is a special case of fragmentation where one of the collision partners has its monomer number conserved. Costas, Moreau and Vicente²⁶ have discussed exact solutions to an extended kinetic Smoluchowski equation which includes cluster disintegration. They also considered the simple scaling of the kernels for the case of constant and additive kernels. Since this is not of primary concern for us here, we refer to their paper for a further discussion.

B. Kernels

In the previous subsection, we discussed the case where the kernels are constant for each cluster size. In practical cases the kernels will be different for each cluster size (and geometry), and each size will be in effect a different species. The kernels entering the Smoluchowski equation have been the subject of active research recently. It can be shown that the scaling properties of the kernels differ for the two families of kinetic models of cluster formation, the *ballistic model* and the *diffusion model* (see Ref. 37 for a discussion and comparison of these two models, as well as an overview of the literature).

Jullien³⁰ has shown that the scaling properties of the kernel for the diffusion model are given by

$$K(i, j) \propto (i^\alpha + j^\alpha)(i^{1/D} + j^{1/D})^{d-2} \quad (2.4)$$

and for the ballistic model by

$$K(i, j) \propto (i^{2\alpha} + j^{2\alpha})^{1/2}(i^{1/D} + j^{1/D})^{d-1}. \quad (2.5)$$

Both expressions scale with cluster size according to the relation

$$K(\lambda i, \lambda j) \propto \lambda^{2\omega} K(i, j), \quad (2.6)$$

where the exponent ω for both the diffusion and the ballistic models is given by

$$2\omega = \alpha + (d - d_w)/D, \quad (2.7)$$

where d_w is the fractal dimension of the cluster trajectory, d is the “true” or embedding dimension (three in this case) and D is the fractal (Hausdorff) dimension of the cluster. For the diffusion case, $d_w = 2$ and for the ballistic case, $d_w = 1$. In the discussion of the Smoluchowski equation given above, the kernels are constant and $\omega = 0$.

We have to determine how the cluster size distribution evolves in time. Jullien *et al.*^{29,30} and Villarica *et al.*²⁵ have shown that for long times the cluster size distribution can generally be written as

$$n_k = Ak^a e^{-b(t)k}, \quad (2.8)$$

where A , a are constants and $b(t)$ is a function of time. From this assumption it follows that²⁵ the scaling behavior of $b(t)$ is given by

$$b \propto t^{1/(2\omega-1)} \quad (2.9)$$

so that the average cluster size $\mu(t)$ scales with time as

$$\mu(t) = \frac{N}{N_C} = \frac{1-2\omega}{b(t)} \propto (t^{1/(2\omega-1)})^{-1} = t^{-1/(2\omega-1)}. \quad (2.10)$$

The value of ω can thus be determined from a fit to the time dependence of μ . From this result and the last equality in Eq. (2.14) it is immediately seen that the total number of clusters $N_C(t)$ scales with time as

$$N_C(t) \propto t^{1/(2\omega-1)}. \quad (2.11)$$

The value of ω is thus an important system parameter, since it characterizes the clustering process almost completely. In the regime $\omega < \frac{1}{2}$ we obtain the *flocculation* regime, which we will restrict ourselves to in our simulations

of gas-phase nucleation. For $\omega > \frac{1}{2}$ we obtain the *gelation* regime, where an infinite cluster appears after a certain characteristic time t_g .

It is interesting to consider the number of clusters n_k with $k > 1$. Initially, n_k must be increasing in time but for large times, the n_k must decrease as the clusters coalesce to form larger clusters. The time t_k at which the maximum in the cluster number n_k appears has been determined by Villarica *et al.*²⁵ and is found to scale with ω as

$$t_k \propto \left(\frac{2-2\omega}{k} \right)^{2\omega-1}, \quad (2.12)$$

which is consistent with the partition into the regimes given above. For $\omega > \frac{1}{2}$ the times t_k are decreasing for increasing cluster size, for $\omega < \frac{1}{2}$ it is an increasing function of k .

C. Moments and distributions

It is convenient to discuss the characteristics of a cluster size distribution over time in terms of its *moments*, which are given by

$$\mathcal{S}_0 = \sum_{i=1}^{\infty} n_i = N_C \quad (\text{Number of clusters}), \quad (2.13a)$$

$$\mathcal{S}_1 = \sum_{i=1}^{\infty} i n_i = N \quad (\text{Number of atoms}), \quad (2.13b)$$

$$\mathcal{S}_2 = \sum_{i=1}^{\infty} i^2 n_i, \quad (2.13c)$$

and in general

$$\mathcal{S}_k = \sum_{i=1}^{\infty} i^k n_i. \quad (2.13d)$$

The equality $\mathcal{S}_1 = N$ follows from the fact that the total number of atoms is conserved and can be used as a check on the programming. In terms of these moments, we can express the average cluster size, $\mu(t)$, as a function of time by

$$\mu_1(t) = \frac{\mathcal{S}_1(t)}{\mathcal{S}_0(t)} = \frac{N}{N_C(t)} \quad (2.14)$$

and the characteristic moments as

$$\mu_i(t) = \frac{\mathcal{S}_i}{N_C}. \quad (2.15)$$

It is convenient to study the time behavior of the cluster formation in terms of the evolution of the log normal distribution of the cluster sizes (see for instance Ref. 38). In this distribution, we assume that n_k is a normal (Gaussian) distribution of the logarithm of cluster size k ($\ln k$).

The moments μ_i can be written in terms of the parameters of the log normal distribution as³⁹

$$\mu_1 = \exp[\overline{(\ln k)} + 0.5\sigma(\ln k)] \quad (2.16a)$$

$$\mu_2 = \exp[2\overline{(\ln k)} + 2\sigma(\ln k)] \quad (2.16b)$$

$$\mu_3 = \exp[3\overline{(\ln k)} + 4.5\sigma(\ln k)] \quad (2.16c)$$

so that we can fit the time development of the characteristics of the log normal distribution from the moments.

Villarica *et al.*²⁵ have investigated the relation between the size distribution in Eq. (2.8) and the log normal distribution and shown that the log normal distribution is a good approximation over a large range of cluster size distributions.

D. The direct Monte Carlo method

The direct Monte Carlo method was initiated by the work of Bird³¹ on fluid structure, and has been used to study model chemical reactions by Anderson.^{32–34}

The central assumption of the DMC method is that the collisions in the gas or fluid are completely random. Therefore we do not have to keep track of the positions of the particles, only their velocities. In contrast to the molecular dynamics methods, we pick colliding pairs randomly. We can simulate a physically sensible number (typically on the order of 10^{23}) of particles by a much smaller amount of particles (on the order of 10^4) if we introduce a simultaneous scaling of their collision cross section. The total Knudsen number remains the same. The main trick of the direct simulation method, as devised by Bird, is that the sampled molecules also serve to evaluate the time-step advance in the simulation. Thus, it is not necessary to evaluate the relative velocities for all possible pairs of molecules. The elimination of the need to track position and the reduction in the number of sample size greatly reduces the computation time required.

The scaling procedure is implemented as follows. If N is the number of physically present particles, V the volume of the cell and N' the number of particles in the simulation, then the scaling of the cross section is given by

$$\sigma'(i,j,v) = \sigma(i,j,v) \frac{N-1}{N'-1}. \quad (2.17)$$

For every collision, the time advance is given by³²

$$\Delta t = \frac{2V}{N'(N'-1)} \frac{1}{(v_{ij}\sigma(i,j))_c}, \quad (2.18)$$

where $(\dots)_c$ designates the quantity for the colliding pair. The cross section for a colliding pair of hard spheres is given as $\sigma(i,j) = \pi r_1^2 (n_i^{1/D} + n_j^{1/D})$.

We define a ‘‘sticking probability’’ $p(i,j)$ for the pair of clusters (i,j) , which gives the probability that they will stick together. The total reactive cross section can then be written in the ‘‘Arrhenius’’ form [see Ref. 15, Eq. (4.17)]

$$\sigma^R(i,j) = p(i,j) \sigma(i,j) \left(1 - \frac{E^*}{E_T} \right), \quad (2.19)$$

for $E_T > E^*$. Here E^* represents the activation energy, E_T the relative translational energy of the cluster pair. When $E_T < E^*$ the reaction probability is zero. The sticking probability is analogous to the steric factor. We can adapt the sticking probability $p(i,j)$ to the situation at hand. Particularly, the sticking probabilities can be made dependent on the cluster sizes according to a power law; we will discuss this in the next subsection.

We introduce a critical cluster size i^* , which is an arbitrary input to our program to determine the course of action if there is no sticking between the clusters. If both cluster i and j have less than i^* monomers, we consider a rearrangement, if at least one of them is larger than the critical cluster size we let them undergo an elastic collision, with a redistribution of the kinetic energy. This is an efficient, albeit somewhat artificial way to introduce the critical cluster size in our simulations: clusters larger than i^* do not break up, on collision they either stick or undergo elastic collisions, whereas clusters smaller than i^* may, on reaction, rearrange their cluster sizes. We neglect breakups into three or more particles.

In the Appendix we discuss the energetics of the collisions, for the types we wish to consider in this paper. We make the assumption that the clusters do not have internal energy modes, hence we neglect energy distributions into rotational and vibrational modes. Though this is a considerable restriction, it is important to note that it is not essential to our model that we make this restriction. The DMC method has sufficient flexibility to include any modes of internal energy distribution if they are known. The binding energy $E_b(k)$ of the cluster k is given in terms of a ‘‘volume’’ term a_V and a ‘‘surface’’ term a_S ^{40,41}

$$E_b(k) = k(a_V - a_S k^{-1/3}), \quad (2.20)$$

where a_V and a_S are constants dependent on the material and k is the number of monomers in the cluster. In our present implementation the binding energy is only used to assess the (energetic) feasibility of a process.

E. Scaling behavior

We can now discuss the use of the DMC method to simulate the Smoluchowski equation. The random choice of the reacting particles accounts for concentration dependence in the rate equation. The product $v_{\text{rel}}(i,j) \sigma_R(i,j)$ is related to the reaction rate constant (and hence to the kernel $K(i,j)$) in the usual fashion¹⁵

$$K(i,j) = k(T)_{ij} = \langle v_{\text{rel}}(i,j) \sigma_R(i,j) \rangle_T. \quad (2.21)$$

The averaging is over the velocity distribution at temperature T . This gives an interesting relation between the kernels and the reactive cross section. Assuming a Boltzmann distribution, the expression for the average velocity of the cluster is

$$v_i \propto \sqrt{\frac{3kT}{m_1 i}}, \quad (2.22)$$

where m_1 is the mass of a monomer and we find that the velocity of the cluster scales with $v_{\lambda i} \propto \lambda^{-1/2} v_i$. The relative velocity also scales with $\lambda^{-1/2}$

$$v(\lambda i, \lambda j)_{\text{rel}} \propto \lambda^{-1/2} v(i,j)_{\text{rel}}$$

and the reduced mass scales with λ

$$\mu(\lambda i, \lambda j) = \frac{\lambda i \lambda j}{\lambda i + \lambda j} \propto \lambda \mu(i,j)$$

so that the total relative kinetic energy $E_T = \frac{1}{2}\mu v^2$ therefore scales as

$$E_T(\lambda i, \lambda j) \propto \lambda^0 E_T(i, j).$$

The cross section $\sigma(i, j)$ scales as $\sigma(\lambda i, \lambda j) \propto \lambda^{2/3} \sigma(i, j)$. The total scaling of the kernel with cluster size is thus given by $2\omega = -1/2 + 2/3 = 1/6$. This result has been obtained earlier^{25,30,42} for ballistic models.

Also of interest is the scaling behavior with temperature. Since $v_i(\lambda T) \propto \lambda^{1/2} v_i(T)$, we have a kernel scaling $K_{\lambda T}(i, j) \propto \lambda^{1/2} K_T(i, j)$. These relationships describe the *dynamical* scaling effects. Deviations from these scalings give specific information about the scaling properties of the nucleating species.

In our model, this is given by the scaling behavior of the sticking probability. Suppose that the sticking probability does not scale with the cluster numbers i and j , but has a constant value p_0 (for instance where p_0 is related to the density of the reactive sites on the surface of the cluster). For a value $p_0 = 1$ and zero activation energy (all collisions resulting in a reaction) the reaction kernel is completely determined by the collision number and we obtain an upper bound to $k(T)$. Conversely, for a low or zero sticking probability where we have a large number of non-reactive collisions, $k(T)$ will be concomitantly lower in this case. However, the same value for ω can be expected, since the scaling behavior essentially remains the same.

We can also make the sticking probability $p(i, j)$ dependent on the cluster numbers i and j . One possibility, which we use in the present paper, is to set

$$p(i, j) = p_0 \times (ij)^{-x}, \quad (2.23)$$

so that the scaling behavior of the sticking probability is given by

$$p(\lambda i, \lambda j) = \lambda^{-2x} p(i, j).$$

We expect a linear dependency of ω on x . The previous case where p_0 is constant corresponds to $x = 0$. We can also simulate the case of a constant kernel. For the ballistic model we have a scaling behavior as above and with the previous expression for the sticking probability we obtain $2\omega \approx 1/6 - 2x$. In the discussion, we will examine a simulation of the Smoluchowski equation with $2x = 1/6$, so that 2ω is zero which is the constant kernel case. The simulation results can then be fitted to Eq. (2.2) and put into Eq. (2.3) to predict the number of clusters as a function of time.

We can obtain ω from the simulation results through the scaling behavior of μ and t_k with ω . In this way, we can relate the very general fractal scaling behavior of the kernels to the underlying physical processes.

III. IMPLEMENTATION

The implementation of the above into a computer program closely follows the initial work of Piersall and Anderson.³² Initially, we let the system consist of only monomers, and we assign velocities to the monomers according to a Maxwell distribution. We then randomly pick

two monomers, compute their relative velocity and cross section and take the product $(v_{\text{rel}}(i, j)\sigma(i, j))$. We take the ratio R of this to the "maximum product" $v\sigma_{\text{max}}$. We compare R to a random number in the set $[0, 1]$ and if R is greater than the random number the pair is accepted for a collision. In this way, we preferentially select pairs with a high $(v_{\text{rel}}(i, j)\sigma(i, j))$. In Anderson's work, the maximum value of $v\sigma$ is chosen as 9/10th of the value obtained in an extended simulation. We have made the following choice. Initially we put the maximum factor to zero. Every computed factor $v(i, j)\sigma(i, j)$ is compared to the current factor $v\sigma_{\text{max}}$. If $(v_{\text{rel}}(i, j)\sigma(i, j))$ is less than $v\sigma_{\text{max}}$, we proceed in the fashion sketched above. If $(v_{\text{rel}}(i, j)\sigma(i, j))$ is greater than $v\sigma_{\text{max}}$ for the current pair, we put

$$(v\sigma_{\text{max}})_{\text{New}} = 2 \times (v_{\text{rel}}(i, j)\sigma(i, j))$$

and we compare the ratio (1/2 in this case) to a random number. If this ratio R is larger than the random number, the pair is accepted for a collision. The pair thus serves to enlarge the value of $v\sigma_{\text{max}}$ and still has a probability of 1/2 to lead to a collision. When the pair collides, we advance the time step and compute the effects of the chemical reaction between the clusters.

For every cluster, we only have to keep track of the total number of monomers in the cluster and its velocity. The cluster cross section can be computed using

$$\sigma(i, j) = \pi(i^{1/D} + j^{1/D})^{d-1},$$

where D is the (fractal) dimension of the cluster and d is the real space dimension. The relative velocity can be computed from the velocities of the individual clusters and the relative translational energy E_T from the relative velocity. After a fixed number of collisions, we write out the values for the time, the averages μ and $S(t)$ and the number of molecules of each cluster species, as well as the moments of the cluster size distribution for later analysis. When a reaction takes place, the number N' is updated. To speed up the program, we also "shrink" the size of the arrays to the current number of clusters after a fixed number of time steps. The total number of particles decreases very rapidly, and the shrinking is needed to avoid too many "misses" in the random selection of colliding monomers.

Our program employs the following units: all distances are expressed in cm, all times in μs , temperature in Kelvin (K) and mass in μ . The implementation of the method is not computation intensive. All calculations were performed on an Apple MacIntosh LC 475 with a Motorola 68040 microprocessor using the MacIntosh Programmer's Workshop Version 3.3.3 and the Absoft FORTRAN compiler Version 3.4. Computation times were on the order of minutes.

IV. RESULTS AND DISCUSSION

In this section, we discuss the simulation results. First, we examine the simulation of the Smoluchowski equation with a constant kernel. We should be able to reproduce the behavior of Eq. (2.2). This will also provide a framework in

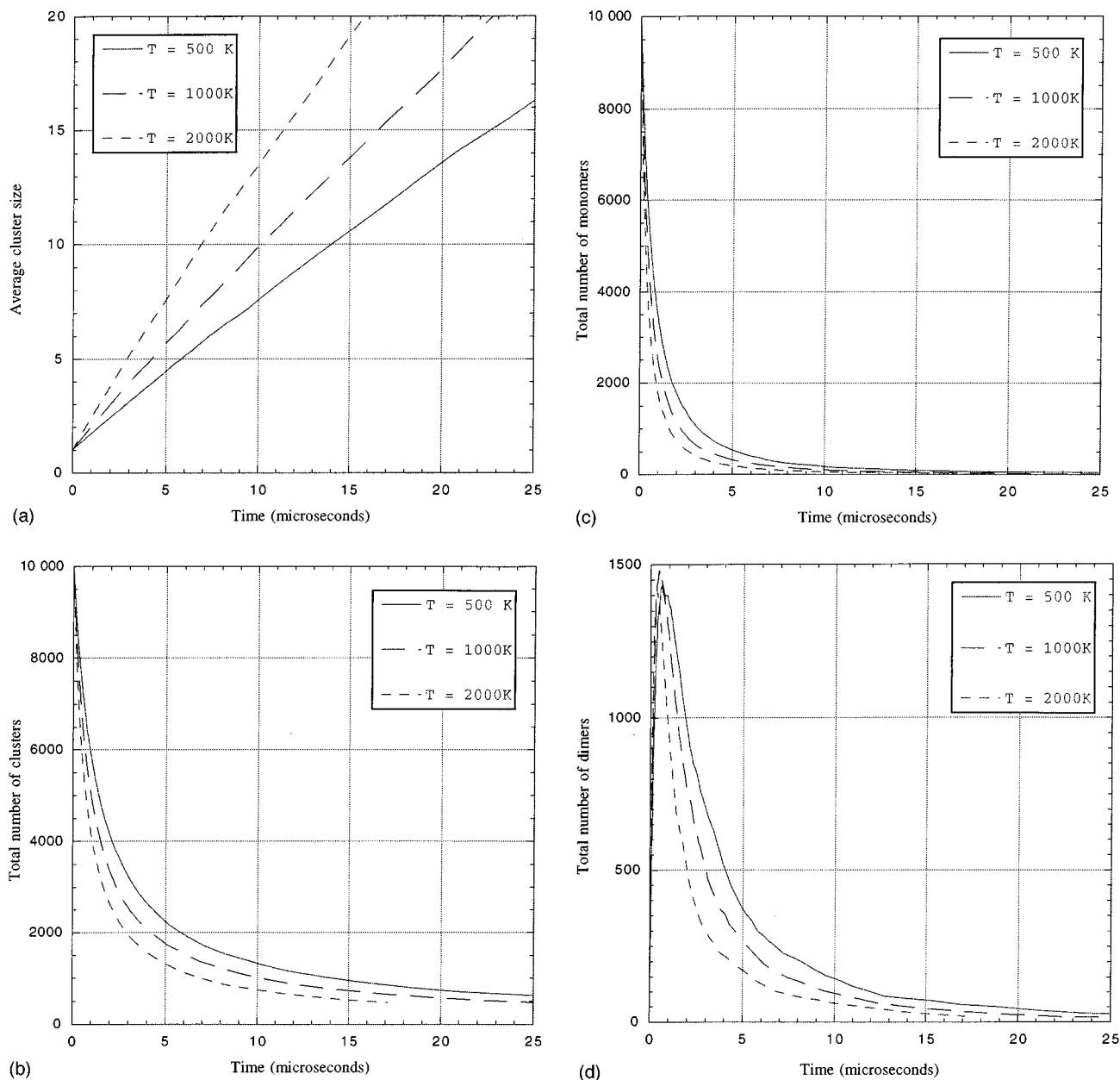


FIG. 1. Immediate simulation of the Smoluchowski equation at temperatures of 500 K, 1000 K and 2000 K. (a) represents average cluster size. Since $\omega=0$ these curves should be straight lines. (b) represents the decrease in the total number of clusters for the three temperatures studied in this section. As can be expected, the decrease is the fastest at the highest temperature. (c) shows the decrease in the monomer concentration. (d) presents the dimer concentration as a function of time for the three temperatures. It is seen that the peak appears later and is somewhat lower with decreasing temperature.

which we can discuss simulations with more complex kernels. Furthermore, we look at simulations with two kinds of models. In the first model, which we call model I, we assume that cluster formation is homogeneous in the kernels. In this model, we also study the possibility that the clusters disintegrate when they are smaller than the critical cluster size. In the second kind, designated model II, we assume anomalously high binding energies and zero sticking probability for clusters of a certain size.

We have adhered to values for the monomer sizes and atomic mass that are consistent with silicon clusters

($m=28u$, and $r=1.17 \text{ \AA}$). We obtained the values for a_B and a_V from a fit to PM3 calculations on the minimum structures of clusters of silicon.⁴³ We employed values of $a_V=-7.7048 \text{ eV}$ and $a_S=-7.6012 \text{ eV}$. The total number of molecules that were simulated was $N=1 \times 10^{16}$, $V=1 \text{ cm}^3$, with a ‘‘real’’ simulated number $N'=10000$. We used $D=d=3$ for the dimensions.

A. Simulation of exact solution

It is possible to simulate the exact solution of the Smoluchowski equation, Eq. (2.2) with our program. To this end

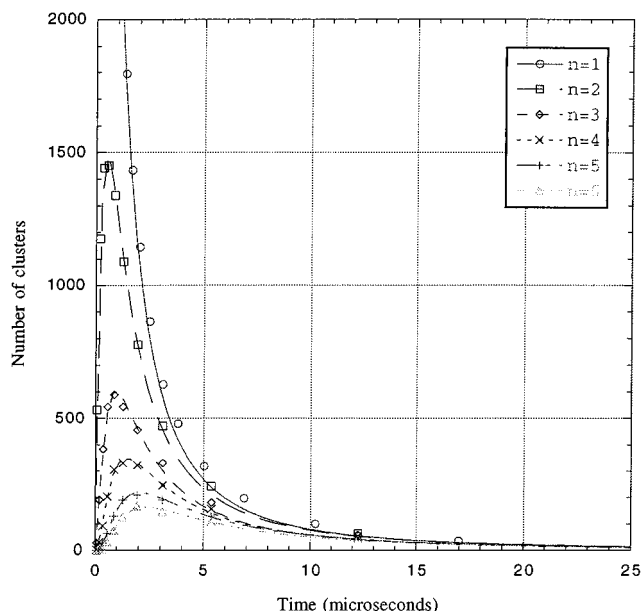


FIG. 2. Display of the time dependence of the cluster concentrations for the first six cluster sizes fitted to exact solutions of the Smoluchowski equation at $T=1000$ K. Here, we have put $2x=1/6$ to obtain a constant kernel and $i^*=0$ to obtain elastic collisions throughout. Points represent simulated results, the curves represent the fits. The numerical fit data are given in Table I.

we set the variables a_V and a_S to zero and we furthermore neglect the possibility of cluster disintegration. We also set the critical cluster size to zero so that all non-sticking collisions are elastic and do not lead to breakups. As noted before, we set $2x=1/6$ ($x=1/12$) to obtain a kernel that is independent of the cluster size. The results form a test of the program and also allow us to assess the precision of the simulation.

In Fig. 1(a) we present the time dependence of the average cluster size as a function of time. A fit to the power law Eq. (2.10) yields values in the range 0.91–0.92 for the exponential dependence, whereas the theoretical value for $\omega=0$ is 1. In Fig. 1(b) we present the total number of clusters as a function of time for three temperatures. At the highest tem-

perature the decrease proceeds most rapidly. Similarly, in Figs. 1(c) and 1(d) we present the time dependence of the monomer and dimer concentrations.

In Fig. 2 we present fits to Eq. (2.2) for 1000 K to the values of k and $(1/2)KN$. The simulation results are represented as dots, the curves represent the fits to the exact equation. The fit is quite good. The fits should reproduce integer values for k and constant values for $(1/2)KN$. The results of the fits for various temperatures are given in Table I where this is seen to be the case to within 10% generally. It can be further noted that the averages of $(1/2)KN$ obey the scaling behavior of K with temperature, as described before: for temperatures twice as large, the value of K should increase with $2^{1/2}$, which is approximately the case.

As well as providing a test of the program, fits to the exact result in Eq. (2.2) provide a useful way to discuss the deviations from the “average” behavior of the clustering process and investigate the effects of various alterations that we can make to the reactive cross sections to make the model more realistic.

B. Model I: Monotonous cluster growth and disintegration

We now consider the monotonous cluster growth model with binding energies dependent on cluster size. The model is simplified in that the effects of internal rotation and vibration are not taken into account.

We choose a parametrization that mimicks the results obtained by Venkatesh *et al.*,³⁵ especially their Figures 11 and 18, where they present the steric factor (“sticking probability”) as a function of cluster size and impact parameter. The sticking probabilities are very small for the small clusters and increase with cluster size until they reach unity for clusters of size 12–14. We model this behavior by choosing $x=-0.4$ and $p_0=0.1$. This leads to a reasonable fit for the cluster monomer sticking probabilities but is only a rough description of the cluster–cluster sticking probabilities. The process is thus characterized by $2\omega=1/6+0.8$. Though this parametrization is the one most consistent with the data provided by Venkatesh *et al.*³⁵ it leads us to a value of ω that is very close to the gelation regime (which appears as a

TABLE I. Simulations of the exact Smoluchowski equation at various temperatures. The results for the first 10 cluster sizes, $1 \leq k \leq 6$ of the simulations with $2x=1/6$ fitted to Eq. (2.2). Both k and $(1/2)KN$ were used as fit parameters. The last line contains the averaged values for $(1/2)KN$ (Avg.).

k	$T=500$ K		$T=1000$ K		$T=2000$ K	
	k_{fit}	$(1/2)KN$	k_{fit}	$(1/2)KN$	k_{fit}	$(1/2)KN$
1	1.0031	0.7159	1.0029	1.0237	1.0013	1.4176
2	2.0111	0.7426	1.9904	0.9973	2.0389	1.5032
3	2.9904	0.7307	3.0546	1.1097	3.0369	1.5536
4	3.9928	0.7409	3.9952	1.0448	3.9516	1.5389
5	4.9872	0.7220	5.0291	0.9906	4.9277	1.3698
6	5.9270	0.6589	5.7968	1.0299	5.8829	1.2562
Avg.		0.7185		1.0327		1.4399

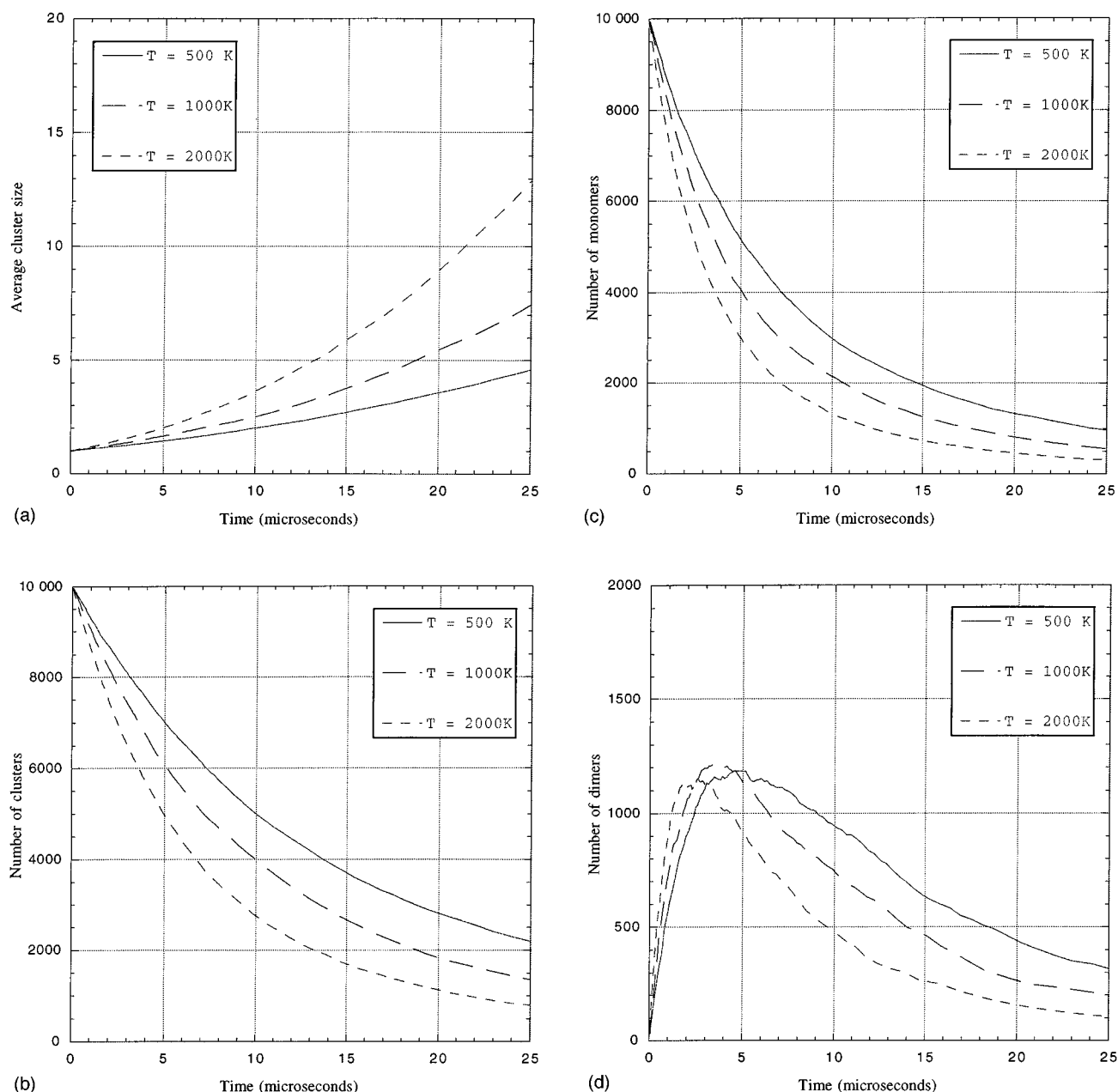


FIG. 3. Average cluster size (a), decrease in the total number of clusters (b), decrease in the monomer concentration (c) and dimer concentrations (d) as a function of time and temperature.

“bumping together” of the maxima in the cluster concentrations) and it is furthermore a value not compatible with the data provided by Villarica *et al.* who have negative values for ω of most materials.²⁵ This suggests that the process of metal cluster formation is not homogeneous in the kernels, at least not with the simple homogeneity suggested by our sticking probability formula.

The results for several temperatures are presented in Figs. 3 and 4. Figure 3 is the counterpart of Fig. 1 and Fig. 4 is the counterpart of Fig. 2. The similarities between the two figures are immediately apparent, so the characterization in terms of the exact Smoluchowski equation is quite accurate in this case. The numerical values of the fits to the size

distributions exhibit large deviations, so the exact solution is only approximately correct in this case. This is no surprise, since the kernel still scales in a homogeneous fashion in this simulation.

We now introduce a critical cluster size, where clusters smaller than the critical cluster size are allowed to disintegrate. We use a distribution which favors splitting a clusters of k monomers into a monomer and a $k-1$ cluster, though other distributions are possible as well. The results of such a calculation are presented in Fig. 5. They are strongly dependent on energetic effects. Line A represents the case of monotonous growth, without disintegration at 1000 K. Line B shows the case where we disintegrate clusters of total size

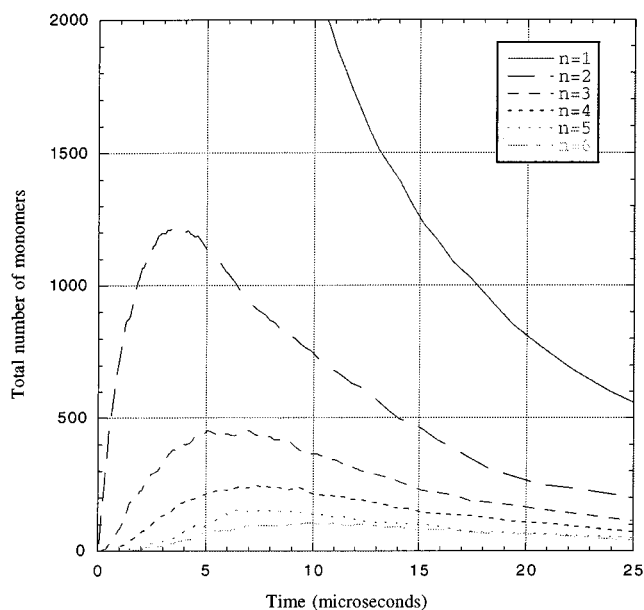


FIG. 4. Concentrations of the $n=2$ – $n=6$ clusters at 1000 K as a function of time.

smaller than 10 monomers and all difference in binding energy (the chemical energy released in the system) is released as kinetic energy of the parts by a scaling of the velocity. Due to the shape of the curve of the binding energy, there is, on average, a small velocity increase with disintegration: at 1000 K, disintegrations that lead to release of energy out-

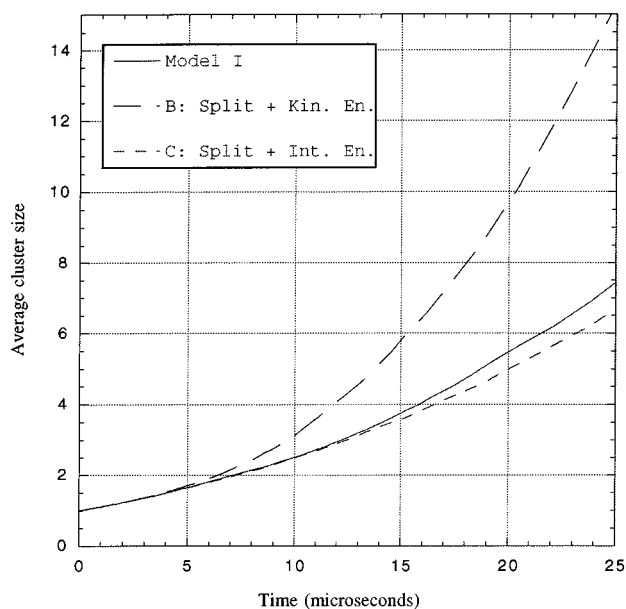


FIG. 5. Average cluster size for cluster formation with various varieties of disintegration of the cluster when the total cluster size is smaller than the critical cluster size. Line A represents the average cluster size without disintegration, line B shows the case where excess binding energy is put into translation, line C the average cluster size with disintegration and “shedding” of the kinetic energy. The “real” average cluster size is somewhere in between lines B and C.

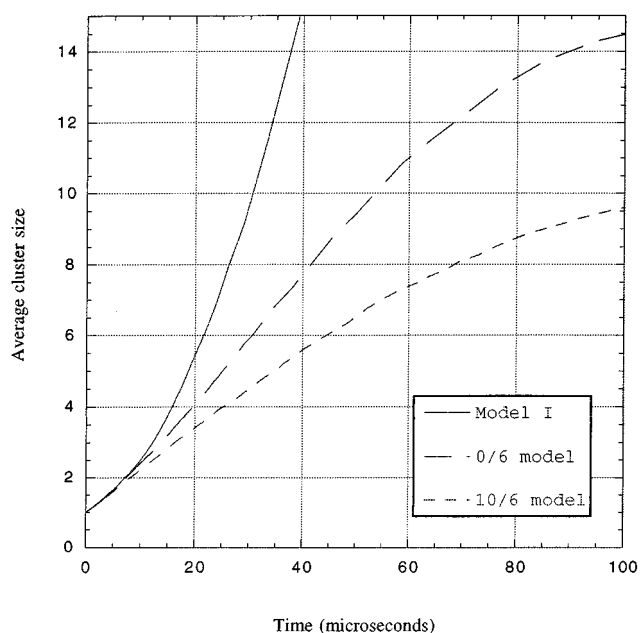


FIG. 6. Average cluster size for cluster formation with anomalously stable clusters (dotted curves) and without such clusters (drawn line). The 0/6 model has an anomalously stable cluster for $n=6$, the 10/6 model adds the effects of cluster disintegration, with shedding of the released binding energy.

number disintegrations that cost energy by about 7 to 1. This leads to an increase in the temperature and hence the speed of cluster formation. Line C shows the case where we do not correct for release of binding energy. If energy is released, it is assumed to disperse into the “internal” modes of the cluster completely. Since we do not know whether the energy release is kinetic or internal, we expect the physical curve to lie between curve B and C. In real cases, the presence of a dilutant gas and the relative effectiveness of heat transfer by different gases would affect the overall temperature and energy distribution in the system.

C. Model II: Supershell clusters

In the formation of clusters, we obtain “anomalous” stabilities for clusters of a certain size. These sizes correspond to “shell closings” in the sense of a “superatom” model. The fact that such clusters are anomalously stable leads to a non-homogeneity in the kernels. We study this effect by arbitrarily making cluster number 6 anomalously stable and chemically inert. Thus the cluster with 6 monomers acts as a “sink” in this simulation. Of special interest are the cluster size distributions.

We present these for a simulation at 1000 K in Figs. 6 and 7. In Fig. 6 we present the average cluster size with the sink cluster (drawn curve) and without the sink cluster (dotted line). The fact that the cluster with six monomers cannot disintegrate, makes the onset of the average cluster size steeper in this case. The fact that it is chemically inert is responsible for the considerable levelling off seen at later times. The fact that the shape of the curve is different in the

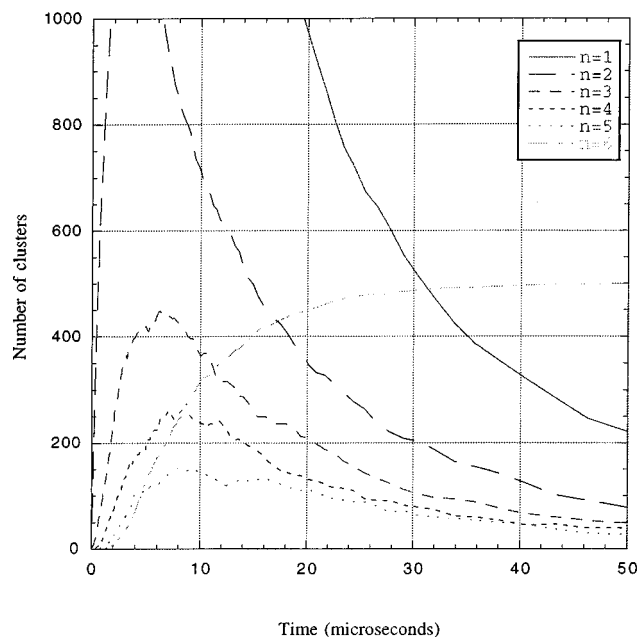


FIG. 7. Cluster size distributions for cluster formation with an anomalously stable cluster at $n=6$. It is seen that the cluster concentration for the anomalously stable cluster steadily grows to a plateau.

case of supershell clusters indicates that supershell behavior can significantly distort the homogeneity of the cluster formation process.

In Fig. 7 we present the cluster size distributions for $n=2$ to $n=6$. It is immediately apparent that the different chemical behavior of the cluster with 6 monomers completely breaks the cluster size distributions which follow from the continuity of the kernels. It is worth while to note that the clusters which do not possess anomalous stability are not affected, a conclusion also drawn by Villarica *et al.*²⁵ The shape of the curve for the stable cluster bears no resemblance to the exact Smoluchowski curve at all.

Anomalous stability for metallic clusters is the rule rather than the exception. We can therefore expect a breakdown of the formulas derived assuming homogeneous kernels in these cases. This questions the use of the single parameter ω for the characterization of metal clustering.

V. CONCLUSIONS

We have initiated the use of the direct Monte Carlo (DMC) method in the study of (metal) cluster formation and have discussed some examples.

We have found the direct Monte Carlo method easy to implement and modify for a host of different physical models that describe cluster chemistry. The method can be easily adapted to incorporate the special effects, such as supershells and anomalous stabilities, which accompany the formation of clusters in the gas phase. Its attractive feature is that the DMC method allows us to focus immediately on the physical aspects of cluster formation, rather than having to make assumptions about the chemical reaction rate constants appearing in the Smoluchowski equation.

The calculations can be easily performed on a personal computer, and in cases where the kernels are homogeneous, the results can be explained in terms of the exact solutions to an approximate Smoluchowski equation. Deviations from this behavior, such as the non-equilibrium properties, the binding energy release when the disintegration is added and the existence of anomalously stable clusters can be easily added to the program. This yields valuable insight into the mechanisms of cluster formation and the possible consequences for applications of this process.

Considerable deviations from idealized behavior appear in the case of an anomalously stable and chemically inert cluster. The appearance of such anomalously stable clusters is very common in the chemistry of metal clusters; considerations such as those of Villarica *et al.*²⁵ which lead to one ω value for every substance should therefore be treated with care.

The DMC method is very well suited to serve as a tool in the study of cluster formation. There is virtually no limit to the detail of the input for example, use of the results from elaborate molecular dynamics and electronic structure calculations.

ACKNOWLEDGMENT

This work was supported by the University of Auckland Research Committee.

APPENDIX: COLLISION TYPES AND ENERGY DISTRIBUTIONS

In this Appendix we discuss the types of collisions and the distribution of the kinetic energies among the particles. We discuss the types of cluster formation mentioned in the introduction to this paper: (i) Simple (elastic) collisions, (ii) stripping or rearrangement, (iii) fragmentation, and (iv) sticking. We neglect three particle breakups, hence (iii).

For the elastic collisions (i), we know the initial velocities and masses of the colliding particles, the other parameters of the collision, notably the impact parameter and the orientation of the closest approach are determined randomly. We use Mintzer's formulas⁴⁴ where the new velocities are related to the centre of mass velocity \mathbf{G} and the new relative velocity \mathbf{g}' by

$$\mathbf{v}'_1 = \mathbf{G} - \left(\frac{m_2}{m_1 + m_2} \right) \mathbf{g}', \quad (\text{A1a})$$

$$\mathbf{v}'_2 = \mathbf{G} + \left(\frac{m_1}{m_1 + m_2} \right) \mathbf{g}'. \quad (\text{A1b})$$

The new relative velocity \mathbf{g}' is given in the laboratory frame by

$$\mathbf{g}' = g \begin{pmatrix} \sin\theta\cos\psi\cos\chi + \cos\theta\cos\psi\sin\chi\sin\epsilon - \sin\psi\sin\chi\cos\epsilon \\ \sin\theta\sin\psi\cos\chi + \cos\theta\sin\psi\sin\chi\sin\epsilon + \cos\psi\sin\chi\cos\epsilon \\ \cos\theta\cos\chi - \sin\theta\sin\chi\sin\epsilon \end{pmatrix}, \quad (\text{A2})$$

where (θ, ψ) represent the spherical coordinates of the relative velocity \mathbf{g} in the lab frame, χ is the angle between the incoming and outgoing velocity vector. We choose χ randomly in the interval $[0, \pi]$ and choose a random value for ϵ in the interval $[0, 2\pi]$.

The other processes have to be treated less deterministically. For a rearrangement (iii) we compute the total of the kinetic and potential energies of the two colliding clusters and distribute the atoms at random in the new clusters. We distribute the fraction of the kinetic energy assigned to the two new clusters in equal portions, and compute new random velocities.

For a reactive sticking collision (iv) we compute the sum of the kinetic energies of the clusters and the excess of binding energy, we form a new cluster and give the velocity of the center of mass of the two initial clusters. We assume that the remainder of the kinetic energy is shed. In fact, this is a simplification, since the new cluster retains its excess energy in rotation or vibration. We furthermore assume that the particle rearranges itself immediately after reaction (on a time scale short in comparison to that of the reaction dynamics) into approximately spherical shape, but retains its excess rotational and vibrational energy.

At present, we do not distinguish between different structures and internal modes of the particles; however, these simplifications are not essential to the method and can be remedied in a more detailed version of the program.

¹W. A. de Heer, *Rev. Mod. Phys.* **65**, 611 (1993).

²M. Brack, *Rev. Mod. Phys.* **65**, 677 (1993).

³E. Haberland and Hellmut, *Clusters of Atoms and Molecules* (Springer Verlag, Berlin, 1994).

⁴T. Kodas and M. Hampden Smith, *The Chemistry of Metal CVD* (VCH, Weinheim, 1994), see p. 488.

⁵G. Selwyn, J. Singh, and R. Bennett, *J. Vac. Sci. Technol. A* **7**, 2758 (1989).

⁶L. Bánjay and S. W. Koch, *Semi-conductor Quantum Dots* (World Scientific, Singapore, 1993).

⁷J. P. Jellinek, in *Metal-Ligand Interactions, Structure and Reactivity*, edited by N. Russo (Kluwer, Amsterdam, 1995), in press.

⁸K. Clemenger, *Phys. Rev. B* **32**, 1359 (1985).

⁹K. Clemenger, *Phys. Rev. B* **44**, 12991 (1991).

¹⁰P. P. Wegener, in *Nonequilibrium Flows*, edited by P. P. Wegener (Marcel Dekker, New York, 1969).

¹¹M. Fisher, *Physics* **3**, 255 (1967).

¹²R. Becker and W. Döring, *Ann. Phys.* **24**, 719 (1935).

¹³M. v. Smoluchowski, *Phys. Z.* **17**, 585 (1917).

¹⁴I. Ford, J. Barrett, and M. Lazaridis, *J. Aerosol. Sci.* **24**, 581 (1993).

¹⁵R. D. Levine and R. B. Bernstein, *Molecular Reaction Dynamics and Chemical Reactivity* (Oxford University Press, New York, 1987).

¹⁶J. L. Katz and M. D. Donohue, *Adv. Chem. Phys.* **40**, 137 (1979).

¹⁷S. L. Girshick and C.-P. Chiu, *J. Chem. Phys.* **93**, 1273 (1990).

¹⁸S. L. Girshick, *J. Chem. Phys.* **94**, 826 (1991).

¹⁹M. Volmer and A. Weber, *Z. Phys. Chem.* **119**, 277 (1926).

²⁰J. Katz, H. Saltsburg, and H. Reiss, *J. Coll. Interf. Sci.* **21**, 560 (1966).

²¹Z. Alexandrowicz, *J. Phys. A* **26**, L655 (1993).

²²W. K. Kegel, *J. Chem. Phys.* **102**, 1094 (1995).

²³H. Hettema and J. S. McFeaters, *J. Chem. Phys.* (to be published).

²⁴M. v. Smoluchowski, *Z. Phys. Chem.* **92**, 129 (1918).

²⁵M. Villarica, M. Casey, J. Goodisman, and J. Chaiken, *J. Chem. Phys.* **98**, 4610 (1993).

²⁶M. E. Costas, M. Moreau, and L. Vicente, *J. Phys. A* **28**, 2981 (1995).

²⁷J. Chaiken and J. Goodisman, *J. Cluster. Sci.* **6**, 319 (1995).

²⁸R. Ball, D. Weitz, T. Witten, and F. Leyvraz, *Phys. Rev. Lett.* **58**, 274 (1987).

²⁹R. Botet, R. Jullien, and M. Kolb, *Phys. Rev. A* **30**, 2150 (1984).

³⁰R. Jullien, *New J. Chem.* **14**, 239 (1990).

³¹G. Bird, *Annu. Rev. Fluid Mech.* **10**, 11 (1978).

³²S. D. Piersall and J. B. Anderson, *J. Chem. Phys.* **95**, 971 (1991).

³³S. D. Piersall and J. B. Anderson, *Chem. Phys. Lett.* **189**, 95 (1992).

³⁴S. M. Dunn and J. B. Anderson, *J. Chem. Phys.* **102**, 2812 (1995).

³⁵R. Venkatesh, R. Lucchese, W. Marlow, and J. Schulte, *J. Chem. Phys.* **102**, 7683 (1995).

³⁶N. Rao and P. McMurry, *Aerosol Sci. Technol.* **11**, 120 (1989).

³⁷P. Meakin, in *The Fractal Approach to Heterogeneous Chemistry: Surfaces, Colloids, Polymers*, edited by D. Avnir (Wiley, New York, 1989).

³⁸C. Wang, R. Huang, Z. Liu, and L. Zheng, *Chem. Phys. Lett.* **227**, 103 (1994).

³⁹G. Herdan, *Small Particle Statistics* (Elsevier, Amsterdam, 1953).

⁴⁰M. Preston and R. Bhaduri, *Structure of the Nucleus* (Addison Wesley, London, 1975).

⁴¹E. Kaxiras and K. Jackson, *Phys. Rev. Lett.* **71**, 727 (1993).

⁴²S. Friedlander, *Fundamentals of Aerosol Behaviour* (Cornell University Press, Ithaca, 1953).

⁴³H. Hettema and J. S. McFeaters (unpublished).

⁴⁴D. Mintzer, in *The Mathematics of Physics and Chemistry*, edited by H. Margenau and G. M. Murphy (Van Nostrand Reinhold, New York, 1964), Vol. 2, Chap. 1.